We are IntechOpen, the world's leading publisher of Open Access books Built by scientists, for scientists

4,800
Open access books available

122,000
International authors and editors

135M
Downloads

Our authors are among the

154
Countries delivered to

TOP 1%
most cited scientists

12.2%
Contributors from top 500 universities

CLARIVATE ANALYTICS BOOK CITATION INDEX INDEXED

WEB OF SCIENCE™

Selection of our books indexed in the Book Citation Index in Web of Science™ Core Collection (BKCI)

Interested in publishing with us?
Contact book.department@intechopen.com

Numbers displayed above are based on latest data collected.
For more information visit www.intechopen.com

Chapter 8

Nanocomposites of Carbon Nanotubes and Semiconductor Nanocrystals as Advanced Functional Material with Novel Optoelectronic Properties

Rima Paul and Apurba Krishna Mitra

Additional information is available at the end of the chapter

http://dx.doi.org/10.5772/66218

Abstract

Semiconductor nanoparticles of very small size, or quantum dots, exhibit fascinating physical properties, completely different from their bulk varieties, mostly because of the quantum confinement effect. Due to their modified band structure, they particularly show attractive optoelectronic characteristics. Carbon nanotubes are a class of nanomaterials, which also possess wonderful optoelectronic properties and can revolutionize modern semiconductor technology to a great extent. Carbon nanotube field-effect transistors (CNTFETs) can replace standard MOSFETs in an array of devices and can function in a more effective way. When these two optoelectronic components combine together in nanocomposites, one may get advanced optoelectronic devices for widespread application in sensors, solar cells, energy storage devices, light-emitting diodes, electrocatalysts, etc.

Keywords: nanocomposites, nanohybrids, quantum dots, carbon nanotubes, optoelectronics

1. Introduction

Advanced research in Materials Science introduced a new direction to control the properties of materials with grain size at nanometer level (1–100 nm). At such reduced scale, materials exhibit fascinating physical properties completely different from their bulk counterparts. The properties of this new class of materials, called nanomaterials, can be tuned by changing their grain size and hence find a wide range of applications. Semiconductor nanoparticles are useful ingredients for the development of optoelectronic devices. This is due to their striking optical and optoelectronic properties, which strongly differ from those of the corresponding bulk

materials. In principle, this is related to the existence of quantum confinement effects of excitons in the nanoparticles. Bandgaps are significantly changed with the size of the nanoparticles, thus modifying the mechanism of radiative recombination of the electrons and holes, which lead to large changes in the emission wavelengths of the excited nanocrystals. Thus, even Si-based nanoelectronic structures may become luminescent with visible light emission, leading to the vast possibilities of optoelectronics [1].

Due to quantum confinement effect, the continuous energy states split into discrete states, with effective blue-shift in the bandgap of the nanomaterials relative to that of bulk materials. Presence of defects such as vacancies, interstitial atoms, surface and grain boundaries in the semiconductor nanocrystals and also doping with appropriate dopants introduce discrete energy levels, which alter the luminescence property of such nanomaterials. An increase in energy bandgap with decrease in particle size leads to a blue-shift in the absorption spectrum. The influence of particle size is found not only in the absorption spectrum but also in the wavelength of the emitted photons. Carbon nanostructures and carbon nanotubes (CNTs), in particular, have such remarkable electronic and structural properties that they are used as active building blocks for a large variety of nanoscale devices. Precisely, the use of carbon nanotubes as active components in electronic and optoelectronic nanodevices has great potential. When nanostructures are synthesized with the hybridization of the above two promising optoelectronic components, a new set of functional nanocomposites appear with fascinating optoelectronic characteristics that may lead to the fabrication of advanced optoelectronic devices for a great variety of potential applications.

2. Quantum confinement in semiconductor nanoparticles

If the size of a nanoparticle becomes comparable to or smaller than the radius of the orbit of the electron-hole pair, then we have a quantum dot (QD) and the case of quantum confinement arises. Quantum confinement can be well explained by applying the laws of quantum mechanics. Quantum confinement is observed in the case of interaction of very small nanocrystals with radiation, when free electrons and holes are created. The hole and the electron form a hydrogen-like system called an 'exciton.' The radius of the exciton, called the 'excitonic Bohr radius,' may range from a fraction of a nanometer to a few nanometers. Quantum confinement occurs when at least one dimension of a nanocrystal is smaller than the diameter of the exciton. In this case, the absorption and emission of light are strongly particle size-dependent and the phenomenon can be explained by the mechanism of quantum confinement. The behavior of subatomic particles is understood by using Schrödinger equation. In a bulk semiconductor, the electrons of the conduction band and the holes of the valence band are free to move throughout the crystal and their motion can be described by the linear combination of plane waves with wavelength of the order of nanometers. Whenever the size of a semiconducting solid becomes comparable to these wavelengths, a free charge carrier confined in this structure will behave as a particle in a potential box. In such a case, the solutions of the Schrödinger equation are standing waves confined within the potential well, and the energies associated with two distinct wave functions are in general different and discontinuous. Thus, the energy of the

http://dx.doi.org/10.5772/66218

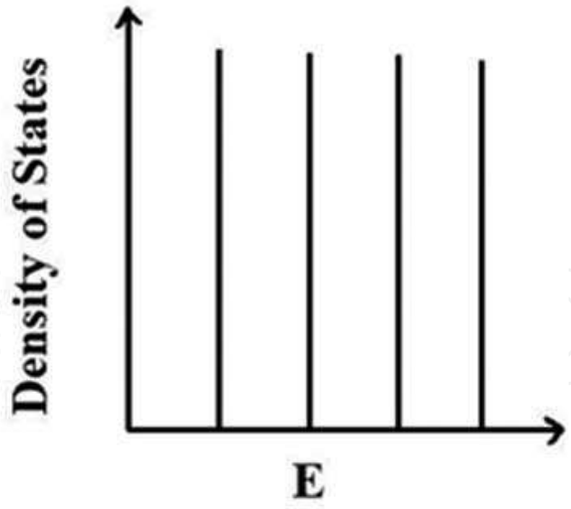

Figure 1. Density of states for a particle in a zero-dimensional nanostructure.

particle exhibits a discrete energy level spectrum. Brus [2] modelled in a simple way the excited electronic states of semiconductor crystallites of sufficiently small size. He expressed the energy of the lowest excited state as:

$$E = \hbar^2\pi^2/2R^2(1/m_e + 1/m_h) - 1.8e^2/\varepsilon_2 R + e^2/Rf(\varepsilon_1, \varepsilon_2) \quad (1)$$

where, R is the radius of the spherical particle with dielectric coefficient, ε_2, which is surrounded by a medium of coefficient, ε_1; E is the shift with respect to the bulk bandgap; m_e and m_h, the effective mass of electron and hole, respectively, and e is the charge of the electron.

In Eq. (1), the second term describes the increase in energy due to confinement effects, while the third term describes the decrease in energy due to Coulomb interaction between electrons and holes.

For a zero-dimensional nanostructure, such as a quantum dot, the density of states is given by:

$$\rho(E)_{0D} = \sum_i 2\delta(E - E_i) \quad (2)$$

where, $\delta(E - E_i)$ is the Dirac δ-function. The density of states for 0D nanostructure is shown in **Figure 1**.

2.1. Optoelectronic properties of QDs

In this section, some significant recent research investigations on the striking optoelectronic properties of semiconductor nanocrystals will be discussed. Liu et al. [3] reported a facile chemical synthesis of SnSe nanocrystals with tunable sizes, by using common alkylphosphine-Se precursors in combination with $SnCl_2$. The optoelectronic properties of colloidal SnSe NCs were studied by fabricating a SnSe NC thin film between interdigitated gold electrodes (**Figure 2(A)**). The current-voltage (I-V) curves were measured in the dark and

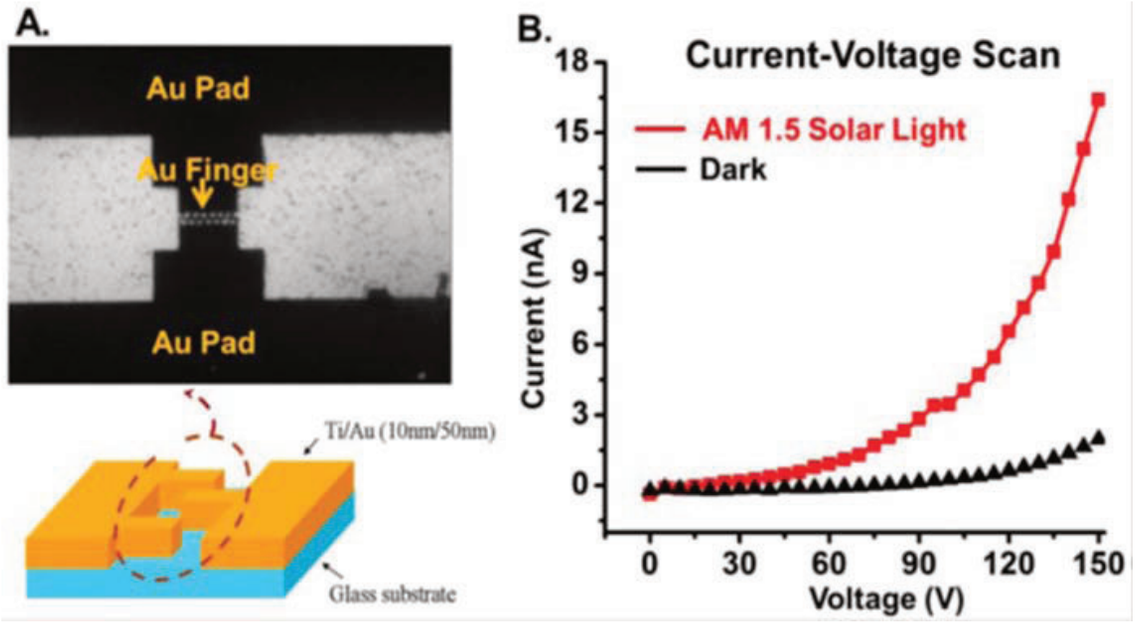

Figure 2. (A) Interdigitated microstructure of metal − semiconductor − metal (MSM) device. (B) Photoresponse of SnSe NC thin-film to AM 1.5 illumination. Reprinted with permission from Liu et al. [3].

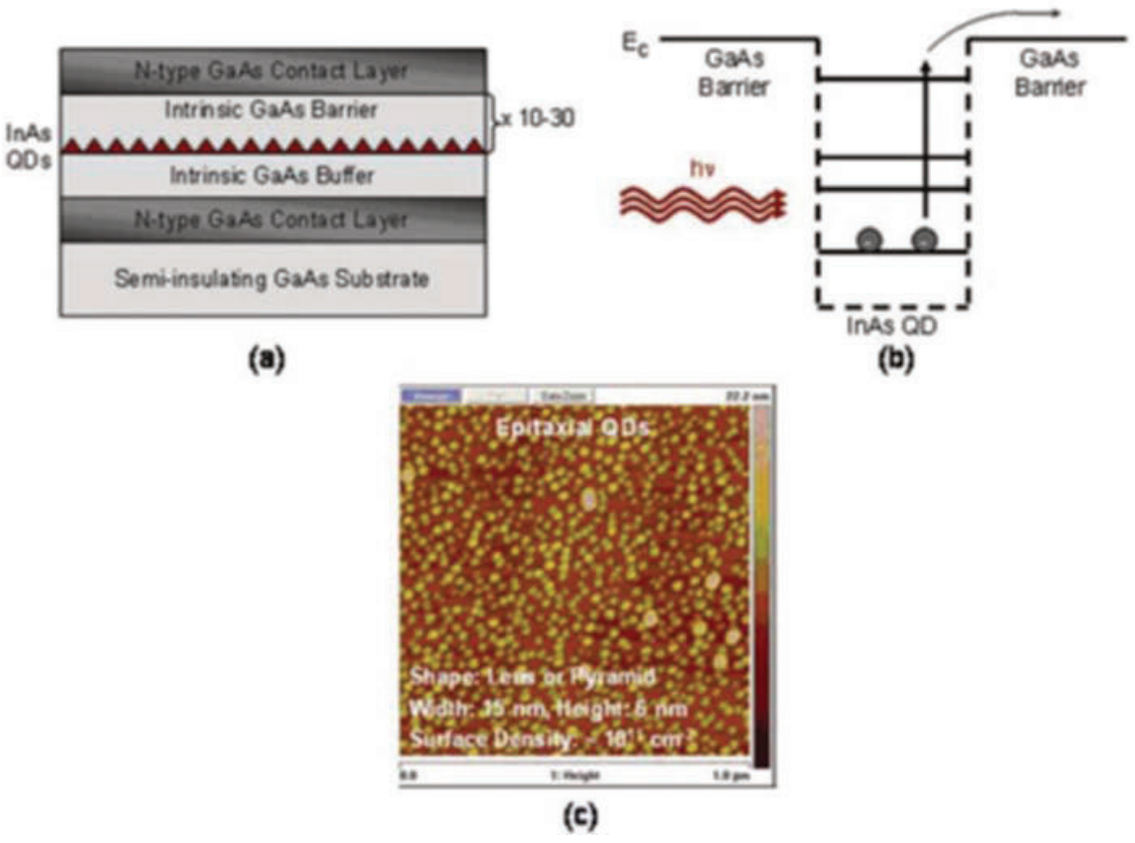

Figure 3. Schematic diagrams of (a) device heterostructure and (b) energy vs. position of intraband transitions demonstrating photocurrent generation in epitaxial InAs/GaAs quantum dot infrared photodetectors. (c) Atomic force microscopy image of epitaxial InAs/GaAs QDs demonstrating important structural characteristics. Reproduced with permission from Stokes et al. [4].

http://dx.doi.org/10.5772/66218

under AM 1.5 simulated solar illumination. The film showed a significant photoresponse (**Figure 2(B)**). The photoresponse of the SnSe nanocrystal thin-film to simulated solar light indicates that the materials have potential for use in solution-processed photovoltaic and optoelectronic devices.

Stokes et al. [4] reported a wet chemical synthesis of semiconductor quantum dots (SQDs), such as cadmium sulphide (CdS) or cadmium selenide (CdSe), etc. They stabilized nanocrystals and controlled their size for specific optical and electronic properties, by chemical capping using some organic capping agent, such as tri-n-octylphosphine oxide (TOPO). They further manipulated their properties by using a core-shell structure of SQDs. Core-shell structures are made by covering the surface of a SQD with a shell of another SQD, which has a greater bandgap than the core (e.g., ZnS over CdS or CdSe). Also as discussed by them, epitaxial quantum dot films (EQDs) of III–V compound semiconductors (InAs/GaAs) have been widely used in infrared photodetectors. **Figure 3** shows the schematics of a typical epitaxial InAs/GaAs infrared photodetector.

3. Carbon nanotubes

The atomic structure of carbon nanotubes depends on tube chirality, which is characterized by the chiral vector $\boldsymbol{C_h}$ and the chiral angle θ. The chiral vector, is defined as a line connecting two crystallographically equivalent sites on a two-dimensional graphene layer, and can be represented in terms of lattice translation indices (n, m) and the basis vectors $\boldsymbol{a_1}$ and $\boldsymbol{a_2}$ as follows:

$$\boldsymbol{C_h} = n\,\boldsymbol{a_1} + m\,\boldsymbol{a_2} \tag{3}$$

where, $n \geq m$ (**Figure 4**).

CNT is constructed by rolling up the graphene sheet such that the two end-points of the vector $\boldsymbol{C_h}$ are superimposed. This CNT is denoted as (n, m) tube with diameter as:

$$D = |\boldsymbol{C_h}|/\pi = a\left(n^2 + nm + m^2\right)^{\frac{1}{2}}/\pi. \tag{4}$$

where $a = |\boldsymbol{a_1}| = |\boldsymbol{a_2}|$ is the lattice constant of the graphene sheet. The tubes with $m = n$ are commonly referred to as armchair tubes, while $m = 0$ as zigzag tube and others having $m \neq n$ are called as chiral tubes. A chiral angle is represented as:

$$\theta = \tan^{-1}\left[3^{1/2}\,m/(m+2n)\right] \tag{5}$$

For an armchair tube, $\theta = 30°$. In the case of a zigzag tube, $\theta = 0°$ and all tubes having chiral angle, $0° < \theta < 30°$, are called chiral tubes. A tube made of a single graphitic layer is called a single-walled carbon nanotube (SWCNT), a tube formed by two coaxial graphitic layers is called a double-walled carbon nanotube (DWCNT), and a tube comprising of several coaxial graphitic cylinders is referred to as a multiwalled carbon nanotube (MWCNT). Through

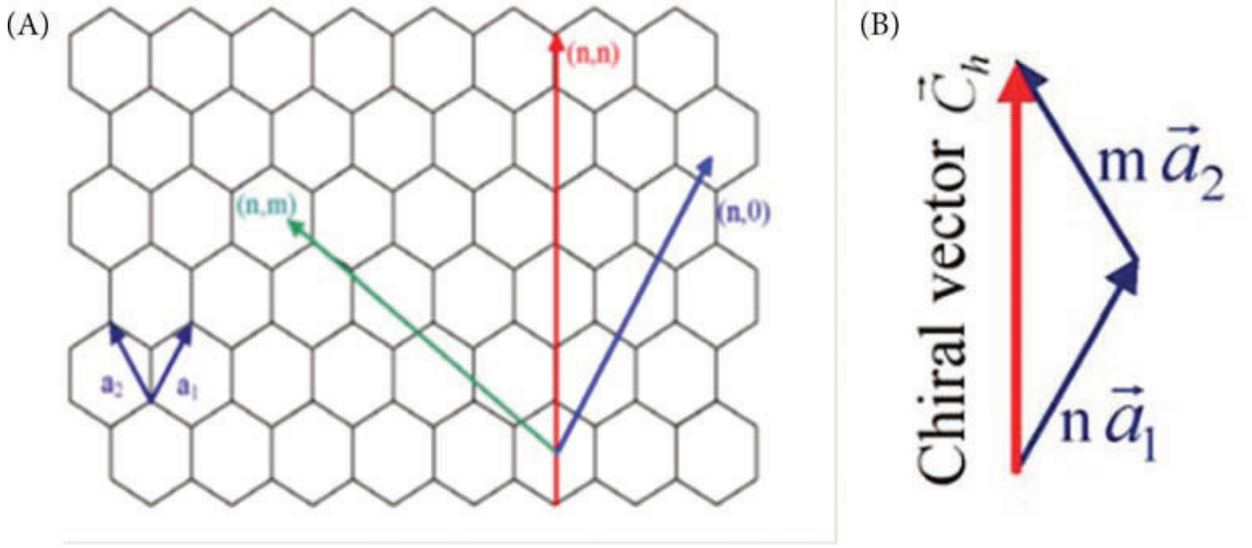

Figure 4. Geometrical structure of carbon nanotubes (CNTs): (A) honeycomb structure and basis vectors, (B) the chiral vector.

theoretical calculations and experimental observations, it has been found that C-C bond length d_{cc} = 0.142 nm or $a = |\boldsymbol{a_1}| = |\boldsymbol{a_2}|$ = 0.246 nm, while the intertube spacing d_{tt} = 0.34 nm in a MWCNT. A carbon nanotube can be semiconducting or metallic depending upon its band structure, which in turn depends on the chirality and diameter of the tube. The electronic structure of the SWCNTs is related to a 2D graphene sheet, but, because of the radial confinement of the wave function, DOS in graphite divides into a series of spikes in SWCNTs (shown in **Figures 5A** and **5B**), which are referred to as van Hove singularities [6]. Density of states gives the number of available energy states and electrons in a given energy interval. For all metallic nanotubes, the density of states per unit length along the tube axis is constant and is given by:

$$N(E_F) = 8/\sqrt{3\pi a\gamma_o} \tag{6}$$

where a is the lattice constant of the graphene sheet and γ_o is the nearest neighbour C-C tight binding overlap energy. The density of states near the Fermi level E_F located at E = 0 for semiconducting nanotubes is zero (**Figure 5A**), but is non-zero and small in the case of metallic nanotubes (**Figure 5B**). Semiconducting nanotubes show that their energy gap depends upon the reciprocal of the nanotube diameter D and is independent of the chiral angle. Thus,

$$E_g = \gamma_o a/\sqrt{3D} \tag{7}$$

Electronic transitions between the energy bands of carbon nanotubes and their standard designations are illustrated in the diagram below for single-walled carbon nanotubes (SWNTs), synthesized in three different techniques, namely hi-pressure carbon monoxide-chemical vapour deposition (HiPCO-CVD), laser ablation, and arc discharge method. Their absorbance characteristics are shown along with following Niyogi et al. [6] (**Figure 5C**).

http://dx.doi.org/10.5772/66218

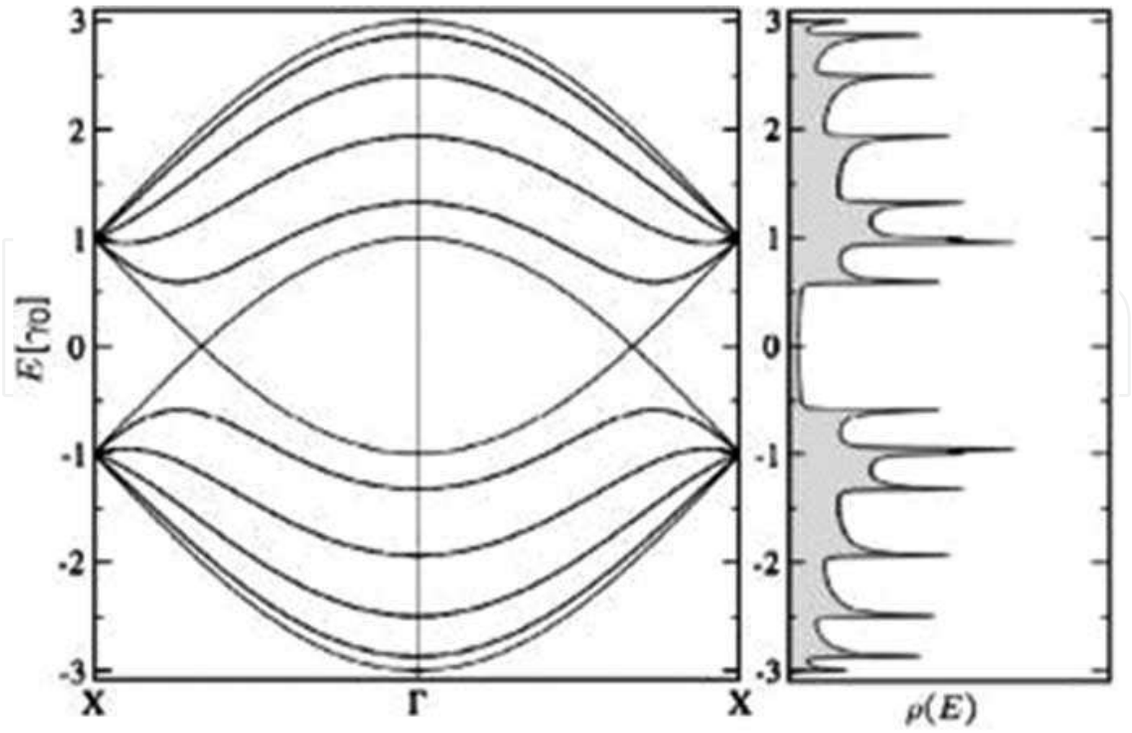

Figure 5A. Band structure and density of states for a (5, 5) armchair nanotube within the zone-folding model. Adapted with permission from Ref. [5].

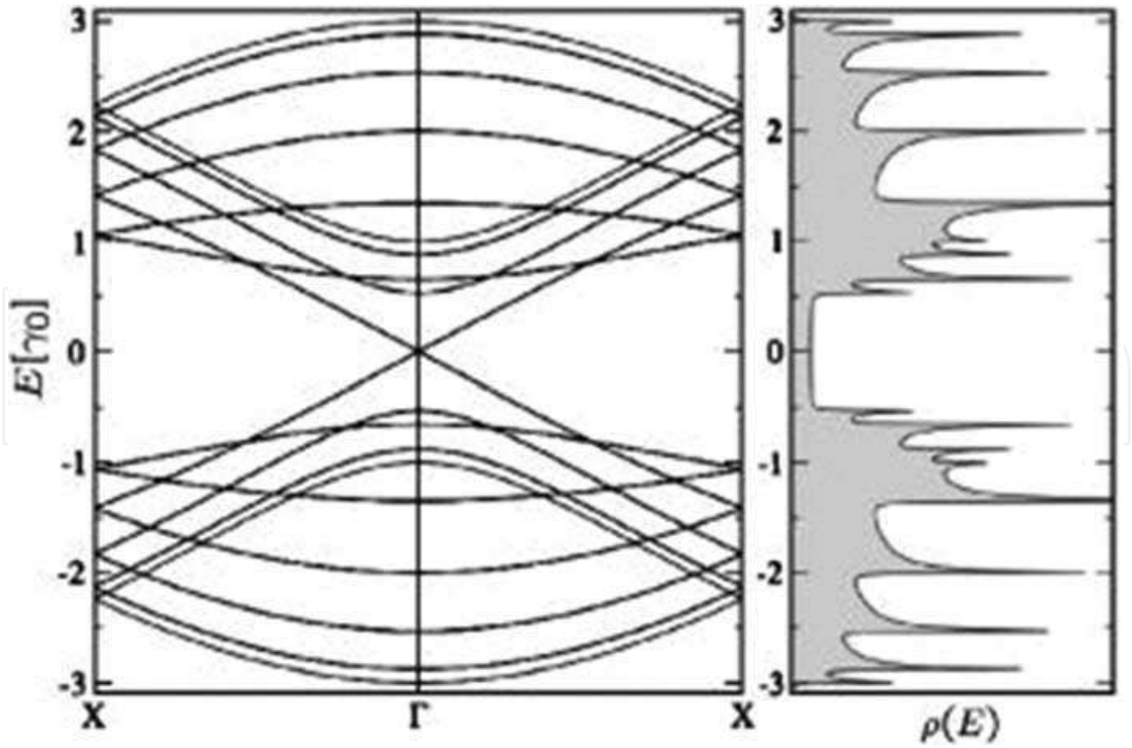

Figure 5B. Band structure and density of states for a (9,0) zigzag nanotube within the zone-folding model. Adapted with permission from Ref. [5].

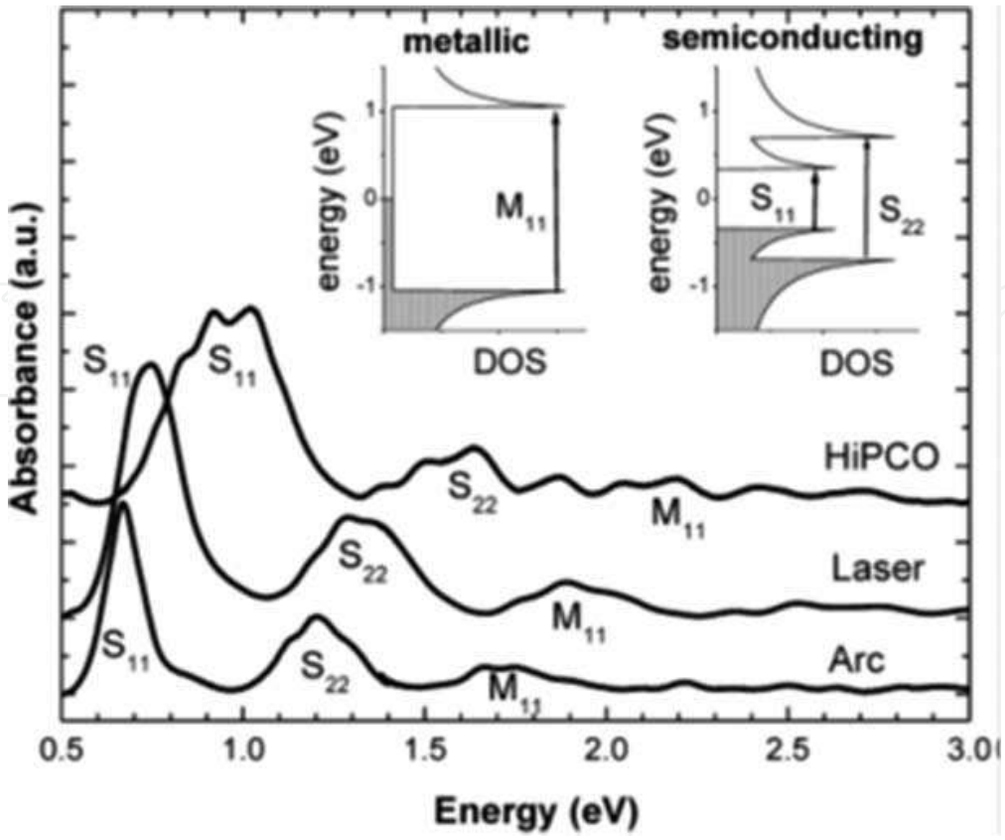

Figure 5C. Electronic transitions between the energy bands of SWNTs, observed by transmission spectroscopy of films, together with a schematic of the nomenclature used to designate the intraband transitions. Reprinted with permission from Ref. [6].

3.1. Optoelectronic properties of carbon nanotubes

A great characteristic of carbon nanotubes is their ability to withstand a very high current density, exceeding 10^9 A/cm^2 [7–9]. For metallic nanotubes, the current-carrying capability may even rise up to a value of 25 μA, limited by Joule self-heating, and by the scattering of optical phonons. The saturation current limit for semiconducting nanotubes is controlled by the Schottky barrier electrical resistance at the nanotube-metal contact, which in turn depends on the diameter of the tube and the work function of the contact metal.

A promising material for fabricating cold cathodes for the next-generation high-performance flat-panel devices is carbon nanotubes (CNTs). Sridhar et al. [10] synthesized a forest of vertically aligned MWCNTs on Inconel 718 substrate and studied its field emission properties. Compared to similar CNT structures grown on silicon, the ones on Inconel substrate were found to possess lower switching fields (~1.5 V/μm), higher operating current (~100 mA/cm^2), and higher amplification factor (~7300), and thus promised enormous potential for use as cold cathodes in microwave vacuum devices, etc. (**Figure 6**).

As explained by Kinoshita [11], a carbon nanotube field-effect transistor (CNTFET) may be designed in a simple way, with the carbon nanotube providing the transport channel when

http://dx.doi.org/10.5772/66218

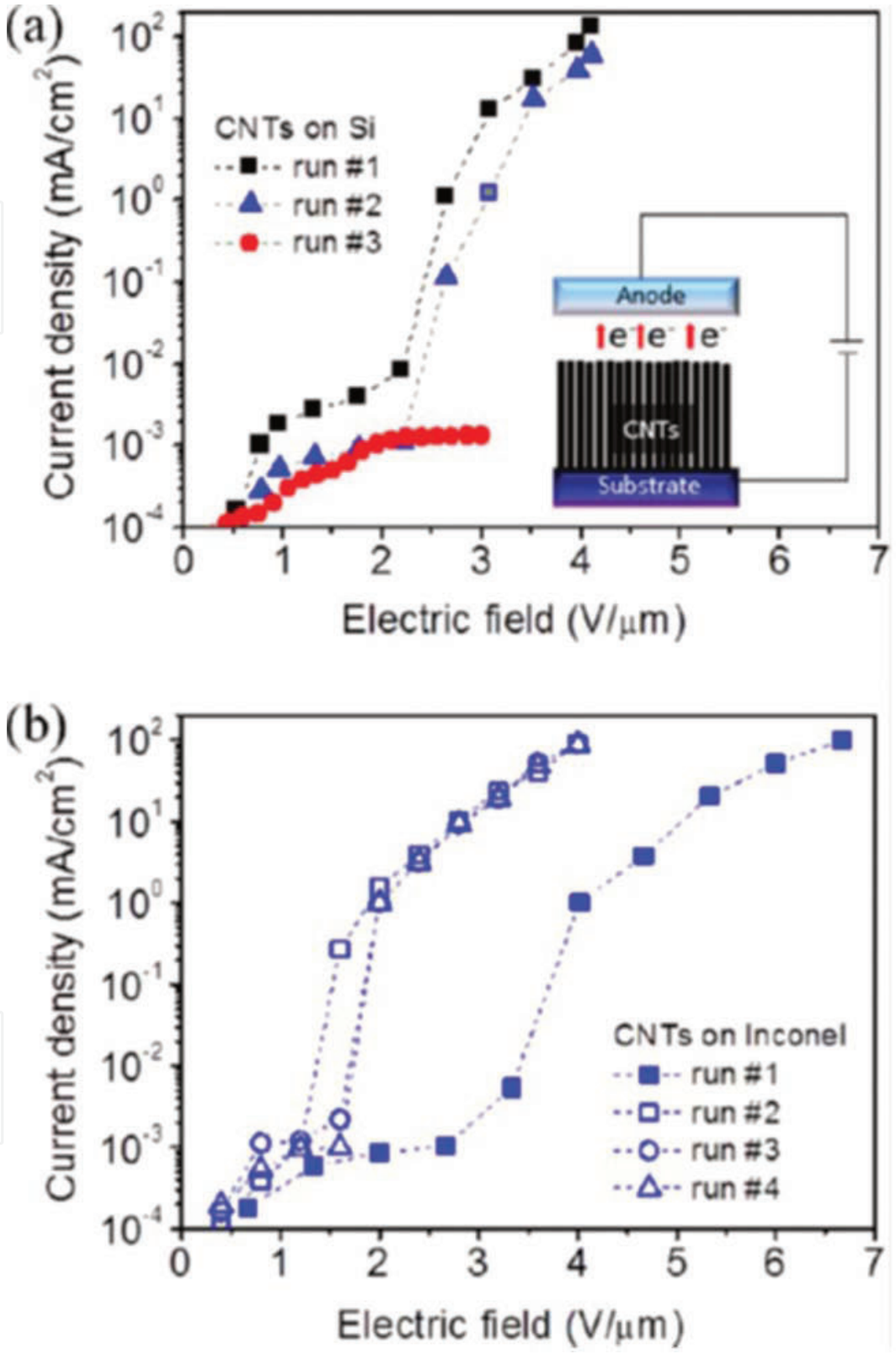

Figure 6. Plots of emission current density as a function of applied electric field in repeated experiments for CNTs grown on (a) Si and (b) Inconel. Reprinted with permission from Ref. [10].

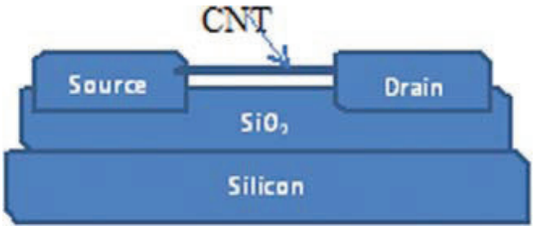

Figure 7. Schematic diagram of a carbon nanotube field-effect transistor (CNTFET).

contacted on each end by bulk metal, and a heavily doped Si substrate acts as the back gate, with SiO_2 performing the function of the gate dielectric. Unlike a conventional MOSFET, a CNTFET operates as a Schottky barrier transistor where the gate controls the Schottky barrier and the injection of carriers. In a CNTFET, one can obtain an I_{on}/I_{off} ratio of 10^5–10^7 and an on-current of ~1 μA at the operating drain-source voltage V_{DS} of 1 V, as observed by Kinoshita [11]. The details of the conduction characteristics depend on the tube diameter, the choice of the contact metal, etc. (**Figure 7**).

Topinka et al. [12] studied carbon nanotube network field-effect transistors (CNTN-FETs). They investigated the microscopic transport mechanism of such devices and observed that in CNTN-FETS the voltage dropped abruptly at a point in the channel where the current was constricted to just one tube. They varied the semiconducting/metallic tube ratio and studied the effect of Schottky barriers on conductance of the channel.

4. Nanoparticle-carbon nanotube composites

When the external surfaces of carbon nanotubes are decorated with semiconductor nanoparticles or quantum dots (NPs/QDs), a new class of functional materials is produced with remarkable properties, which combine the unique characteristics of the individual components. Such nanostructures are known as CNT-NP (or CNT-QD) hybrids, or nanocomposites. These nanocomposite materials are potentially useful in a wide range of advanced applications, in the field of chemical sensors [13], biosensors [14], electrocatalysis [15], fuel cells [16], and nanoelectronics [17]. Semiconductor NPs of very small size are known as quantum dots (QDs), as they exhibit interesting size-dependent optical and electronic properties, due to quantum confinement effect. As observed by Georgakilas et al. [18] CNTs hybridized with QDs of II–VI or III–V semiconductors are ideal optoelectronic materials and can be used in solar cells, light-emitting diodes, etc.

Therefore, varieties of semiconductor NPs, such as CdSe, CdS, CdTe, PbSe, ZnS, ZnO, SiO_2, TiO_2, and In_2S_3, have been bound to CNT surfaces and properties studied by several researchers.

The electronic interaction between CNTs and the externally attached nanocrystals (NCs) plays a crucial role in constructing optoelectronic devices [19, 20]. Hybridizing semiconductor NPs on CNT surfaces can modify their optical characteristics and luminescent property significantly and hence can find application in assembling photoelectrochemical cells [21], in tailoring

http://dx.doi.org/10.5772/66218

light-emitting diodes [22], in organizing sensor systems, and in fabricating electrochromic devices [23].

4.1. Synthesis and characterization of the CNT-QD composites

There are several methods to decorate carbon nanotubes with nanoparticles. Chen and Lu [24] proposed an efficient gas-phase route of the electrostatic force directed assembly (ESFDA) process. The locally enhanced electric field near CNTs results in directed assembly of charged aerosol nanoparticles onto CNTs. They coated MWCNTs with a mixture of SnO_2 and Ag nanocrystals by using this method.

However, the most widely exploited route for synthesis of semiconductor nanoparticle-coated carbon nanotubes is the wet chemical process. In this method, the size of the QDs can be tuned and the proportions of the two components of the composite can be adjusted to obtain the desired properties. Carboxyl groups on the surface of acid-treated CNTs are often used to attach amine-terminated or mercapto-terminated inorganic nanoparticles through amide bonds.

Banerjee and Wong [25] used a multistep procedure to attach modified CdSe QDs to carboxyl-group functionalized CNTs (**Figure 8**).

Li et al. [26] used polyamine- and amino-functionalized MWCNTs (MWCNT-NH_2) templates to load CdTe quantum dots (QDs) and Fe_3O_4 magnetic nanoparticles by the electrostatic self-assembly approach, synthesizing MWCNT/CdTe and MWCNT/Fe_3O_4 nanohybrids (**Figure 9**).

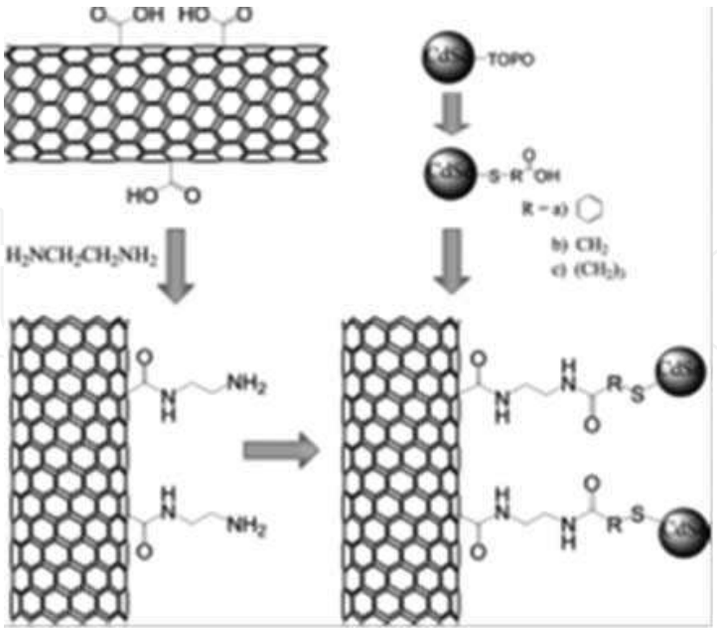

Figure 8. Multistep process for linking modified CdSe QDs to CNTs via amide bonds, involving (1) the oxidation of CNTs in $KMnO_4$ and functionalization with ethylenediamine and (2) the thiolization of CdSe and termination with acid groups. Reprinted with permission from Ref. [25].

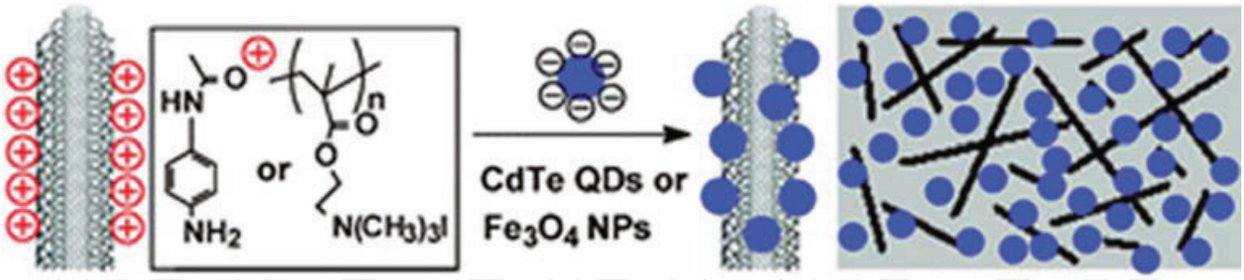

Figure 9. Synthesis procedure for preparation of MWCNT/nanoparticle hybrids from multiamino-functionalized MWCNTs by the electrostatic self-assembly approach. Reprinted with permission from Ref. [26].

Robel et al. [27] investigated the single-walled carbon nanotube-CdS nanocomposites as light-harvesting assemblies and studied their photoinduced charge-transfer interactions, undertaking a simple solution-mixing synthesis of the samples as shown in **Figure 10**.

Paul et al. [28] reported a simple chemical precipitation technique for the synthesis of a hybrid nanostructure of single-wall carbon nanotubes (SWCNT) and titania (TiO_2) nanocrystals of average size 5 nm (**Figure 11**). They prepared SWCNT/TiO_2 nanohybrid structures by mixing purified SWCNT in $TiCl_3$ solution and stirring the mixture in a magnetic stirrer. NH_4OH solution was added in drops to attain pH neutrality and the mixture was further stirred for a few hours. Then, they centrifuged the colloidal solution at 9°C, washed it with deionized water and 2-propanol, and dried up at room temperature. They did structural and morphological characterization of the samples, and studied their optical and electrical properties.

In the absorbance spectra of the nanohybrid material, a blue-shift was observed by them, confirming the charge transfer between SWCNTs and titania nanoparticles. There was a

Figure 10. Chemical synthesis of SWCNT/CdS hybrid structure in THF solution is shown on the right part of the figure. The different stages of formation of the nanocomposite are shown in a labelled flowchart. The left part shows the charge transfer mechanism between excited CdS nanoparticles and SWCNTs. Reproduced with permission from Ref. [27].

http://dx.doi.org/10.5772/66218

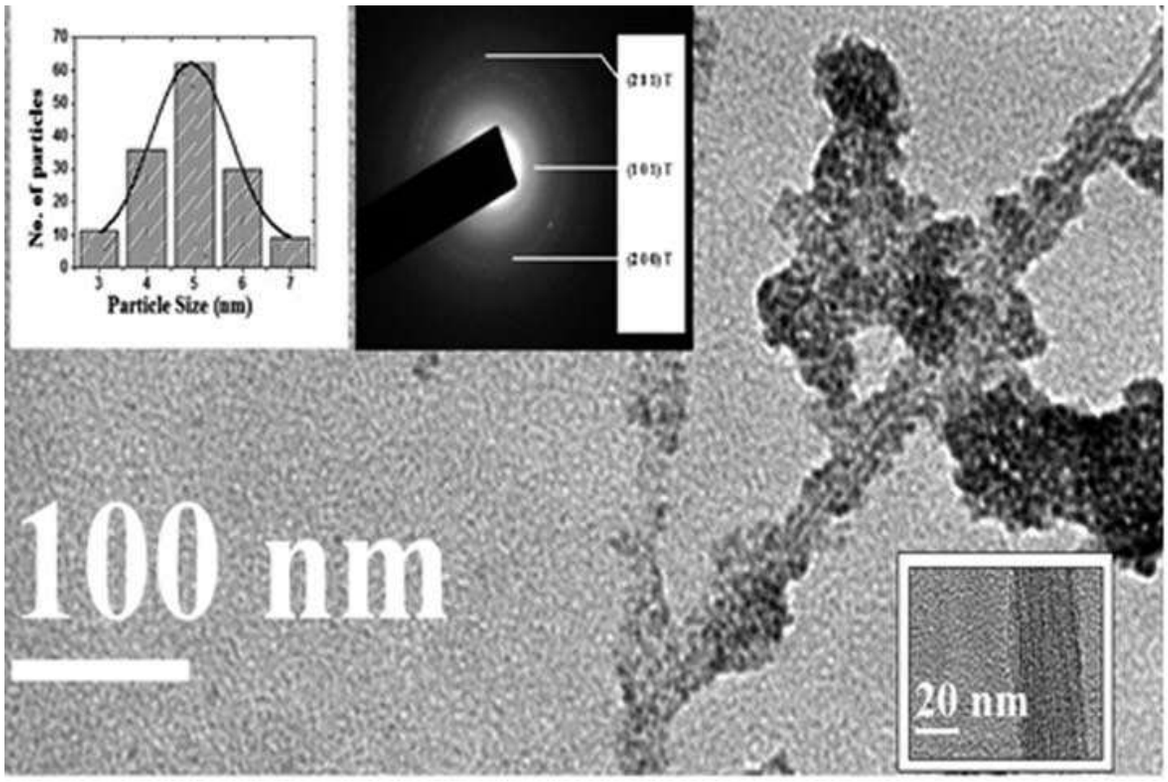

Figure 11. HRTEM micrograph of SWCNT/TiO_2 hybrid; insets showing the HRTEM micrograph of pristine SWCNT, SAED pattern of the composite material and the particle size distribution of TiO_2 NCs. Copyright © 2013 Techno-Press, Ltd.

considerable visible emission in the photoluminescence spectrum with the peak emission at 400 nm.

Figure 12 shows the Raman spectrum of pristine SWCNT and that of SWCNT/TiO_2 hybrid. The peaks at 150, 408, and 650 cm^{-1} of the hybrid sample correspond to the photoelectronically active TiO_2 anatase phase. There is an upshift by 12 cm^{-1} in the position of G-band indicating charge transfer to SWCNTs from TiO_2 NCs. I_D/I_G for pristine SWCNT was 0.546, while that for SWCNT/TiO_2 hybrid was found to be 0.939.

Study of DC conductivity of pristine SWCNT showed a crossover from a semiconductor-like temperature dependence of conductivity to a metal-like one with the increase of temperature, transition temperature being 180 K (**Figure 13**). When coated with TiO_2 NPs, the whole material behaves as a semiconducting material and its conductivity decreases by several orders of magnitude. A broad luminescence in the visible region in the range of 325–500 nm was observed, which could be attributed to the charge transfer from the titania NCs to the SWCNTs. Thus, the hybridization of TiO_2 nanoparticles with SWCNTs rendered an advanced functional material with improved photocatalytic response due to reduced recombination of photoelectrons. Also, this nanocomposite could find application as a useful optical material for sensor devices.

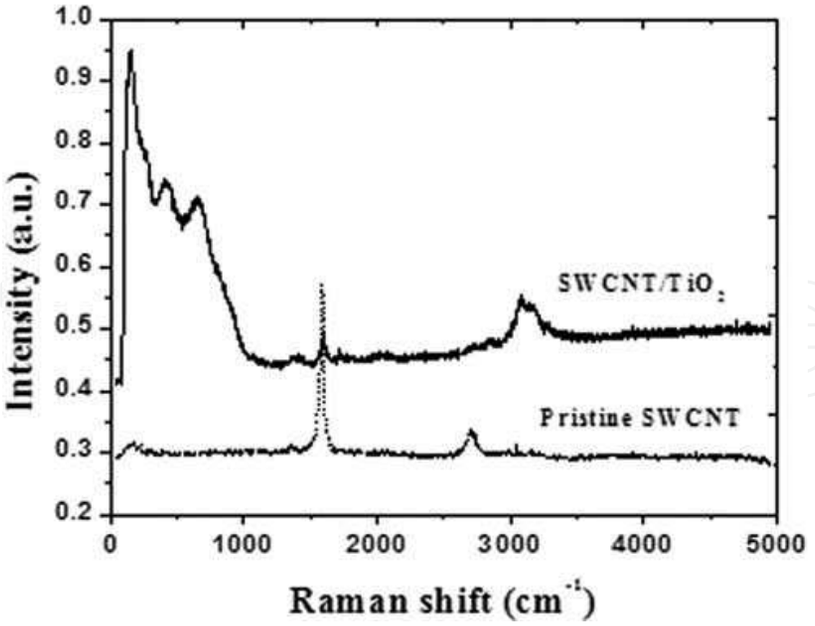

Figure 12. Raman spectrum of pristine SWCNT and SWCNT/TiO_2 composite. Copyright © 2013 Techno-Press, Ltd.

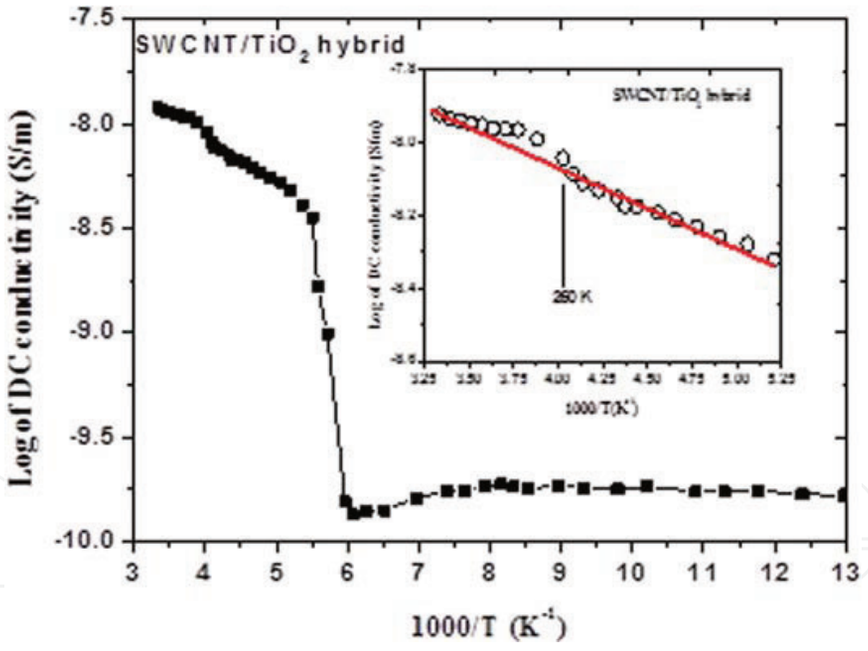

Figure 13. Variation of log of DC conductivity of SWCNT/TiO_2 hybrid with 1000/T (K^{-1}); inset shows the higher temperature plot of DC conductivity of the hybrid. Copyright © 2013 Techno-Press, Ltd.

4.2. Optoelectronic applications of CNT-QD composites

Yang et al. [29] synthesized In_2S_3-carbon nanotube nanocomposites through a facile refluxing wet chemistry process, as shown in the migrograph (**Figure 14**). The as-synthesized In_2S_3-CNT nanocomposites were used as selective and active visible-light driven photocatalysts toward

http://dx.doi.org/10.5772/66218

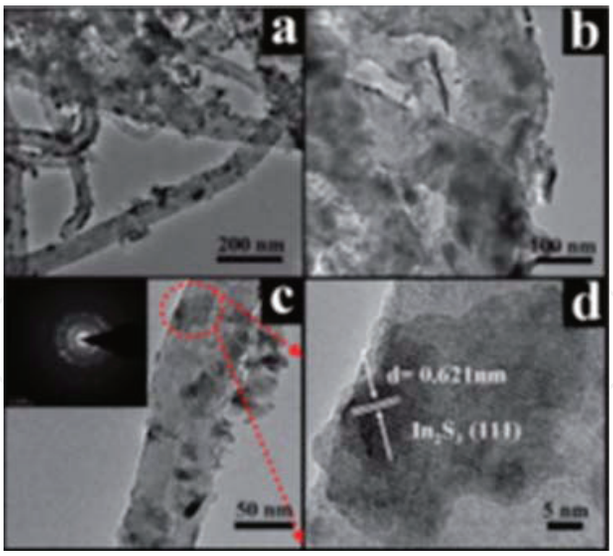

Figure 14. Typical TEM images (a–c) and high-resolution TEM (HR-TEM) image (d) of the sample of In_2S_3-3% CNT; the inset of panel (c) is the corresponding SAED pattern. Reprinted with permission from Ref. [29].

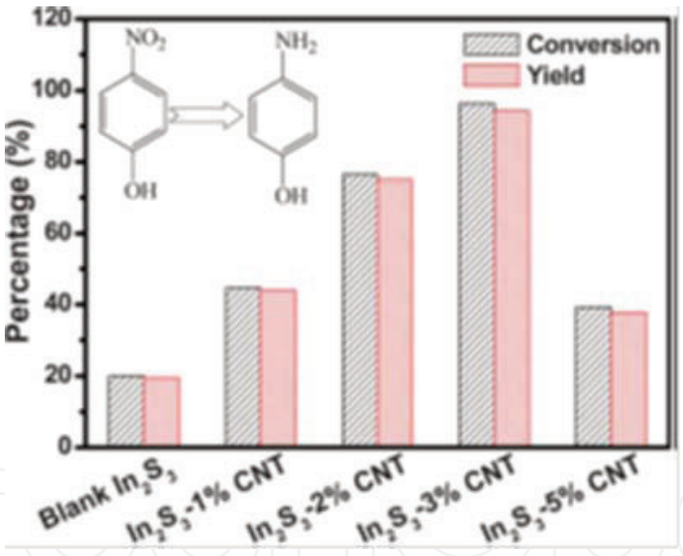

Figure 15. Photocatalytic selective hydrogenation of 4-NP over blank In_2S_3 and In_2S_3-CNT nanocomposites under visible light irradiation for 1 h in water with the addition of ammonium formate as a hole scavenger and N_2 purge at room temperature. Reprinted with permission from Ref. [29].

hydrogenation of nitroaromatics to amines in water, with enhanced photocatalytic performance (**Figure 15**).

Shi et al. [30] reported a simple process for the synthesis of a sandwich structure of SWCNT-CdSe hybrid film (thickness ~ 200 nm), in between two SWCNT films (each thickness ~ 36 nm). They tested it as an optoelectronic conversion device under the illumination of simulated solar

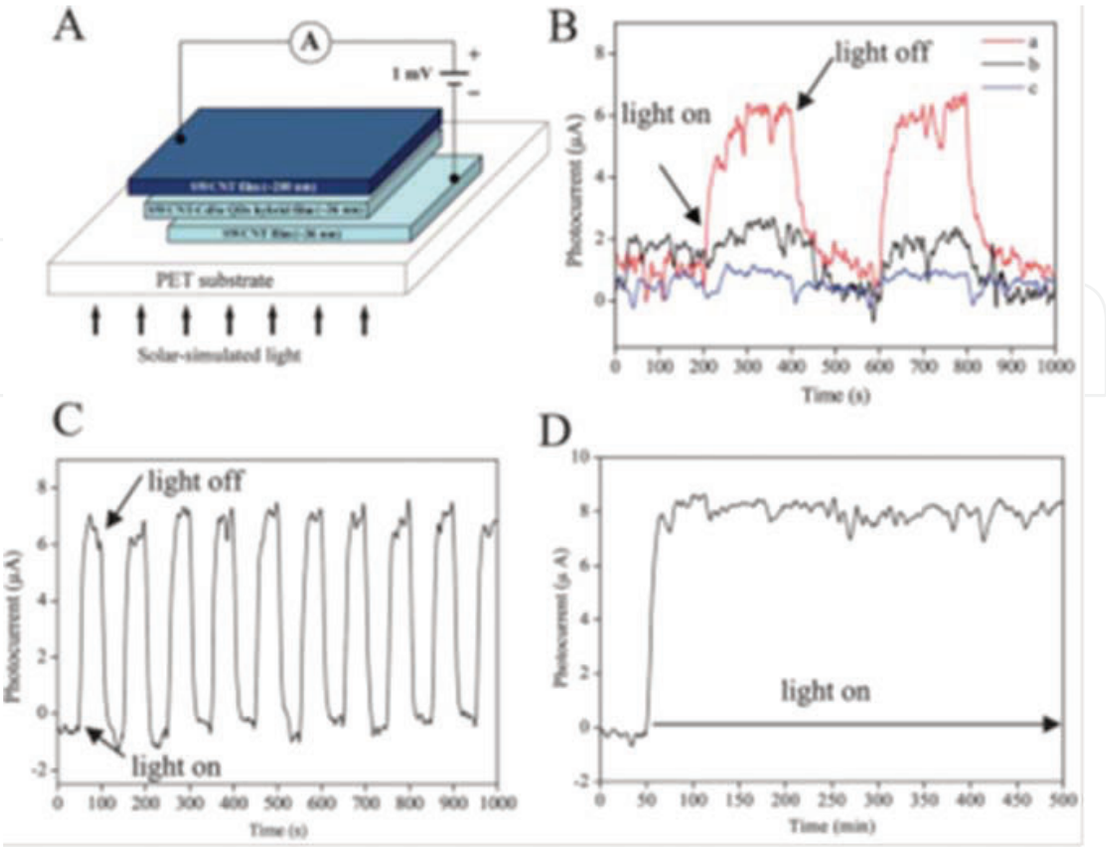

Figure 16. (A) Schematic diagram of an optoelectronic device using SWCNT-CdSe hybrid film. (B) Photocurrent vs. time under alternating light on and light off condition (a) for the device using calcined SWCNT-CdSe film as the middle layer. Curve (b) is for the device using SWCNT-CdSe film without calcination. Curve (c) is for the device using pure SWCNT film. (C) On/off light cycles of photocurrent and (D) photocurrent for a long-time illumination with light of 100 mW cm^{-2}. Reproduced with permission from Shi et al. [30].

light. They found that the device could generate photocurrent with high sensitivity and their observations are illustrated in **Figure 16**.

5. Conclusion

Attachment of semiconductor nanoparticles or quantum dots on the surfaces of carbon nanotubes has opened up innumerable possibilities of their applications in a variety of advanced nanodevices in various areas of nanotechnology. Combining the remarkable opto-electronic properties of the two outstanding nanoscale components, a vast array of fascinating optoelectronic devices is being proposed by researchers every day all over the world. In our brief review, we have touched upon a few of such applications.

Acknowledgment

One of the authors (Rima Paul) is indebted to Dr. D. S. Kothari Foundation for supporting her through Dr. D. S. Kothari Post Doctoral Fellowship at Indian Institute of Science, Bangalore, India.

Author details

Rima Paul[1] and Apurba Krishna Mitra[2,3]*

*Address all correspondence to: akmrecdgp@yahoo.com

1 Materials Engineering Department, Indian Institute of Science, Bangalore, India

2 Department of Physics, National Institute of Technology, Durgapur, India

3 Presently retired

References

[1] Gonzalez-Varona O, Perez-Rodrõguez A, Garrido B, Bonafos C, Lopez M, Morante JR, Montserrat J, Rodrõguez R. Ion beam synthesis of semiconductor nanoparticles for Si-based optoelectronic devices. Nuclear Instruments and Methods in Physics Research B. 2000; 161–163: 904–908.

[2] Brus LE. Electron-electron and electron-hole interactions in small semiconductor crystallites: The size dependence of the lowest excited electronic state. The Journal of Chemical Physics. 1984; 80: 4403–4409. DOI: 10.1063/1.447218

[3] Liu X, Li Y, Zhou B, Wang X, Cartwright AN, Swihart MT. Shape-controlled synthesis of SnE (E = S, Se) semiconductor nanocrystals for optoelectronics. Chemistry of Materials. 2014; 26: 3515–3521. DOI: 10.1021/cm501023w

[4] Stokes EB, Stiff-Roberts AD, Dameron, CT. Quantum dots in semiconductor optoelectronic devices. The Electrochemical Society Interface Winter. 2006; 15(4).

[5] Charlier JC, Blase X, Roche S. Electronic and transport properties of nanotubes. Reviews of Modern Physics. 2007; 79: 677–732. DOI: 10.1103/RevModPhys.79.677

[6] Niyogi S, Hamon MA, Hu H, Zhao B, Bhowmik P, Sen R, Itkis ME, Haddon RC. Chemistry of single-walled carbon nanotubes. Accounts of Chemical Research. 2002; 35: 1105–1113. DOI: 10.1021/ar010155r

[7] Collins PG, Arnold MS, Avouris P. Engineering carbon nanotubes and nanotube circuits using electrical breakdown. Science. 2001; 292(5517): 706–709. DOI: 10.1126/science.1058782

[8] Wei Y, Xie C, Dean KA, Coll BF. Stability of carbon nanotubes under electric field studied by scanning electron microscopy. Applied Physics Letters. 2001; 79(27): 4527–4529. DOI: 10.1063/1.1429300

[9] Yao Z, Kane CL, Dekker C, High-field electrical transport in single-wall carbon nanotubes. Physical Review Letters. 2000; 84(13): 2941–2944. DOI: 10.1103/PhysRevLett.84.2941

[10] Sridhar S, Ge L, Tiwary CS, Hart AC, Ozden S, Kalaga K, Lei S, Sridhar SV, Sinha RK, Harsh H, Kordas K, Ajayan PM, Vajtai R. Enhanced field emission properties from CNT arrays synthesized on inconel superalloy. ACS Applied Materials & Interfaces. 2014; 6: 1986–1991. DOI: 10.1021/am405026y

[11] Kinoshita M. *Optoelectronics with Carbon Nanotubes*, Ph.D. Dissertation, State University of New York at Stony Brook: 2011; pp. 15–17.

[12] Topinka MA, Rowell MW, Goldhaber-Gordon D, McGehee MD, Hecht DS, Gruner G. Charge transport in interpenetrating networks of semiconducting and metallic carbon nanotubes. Nano Letters. 2009; 9(5): 1866–1871. DOI: 10.1021/nl803849e

[13] Kong J, Chapline MG, Dai HJ. Functionalized carbon nanotubes for molecular hydrogen sensors. Advanced Materials. 2001; 13: 1384–1386. DOI: 10.1002/1521-4095(200109)13

[14] Chen RJ, Bangsaruntip S, Drouvalakis KA, Kam NWS, Shim M, Li YM, Kim W, Utz PJ, Dai HJ. Noncovalent functionalization of carbon nanotubes for highly specific electronic biosensors. Proceedings of the National Academy of Sciences, 2003 USA. 2003; 100: 4984–4989. DOI: 10.1073pnas.0837064100

[15] Luo J, Jones VW, Maye MM, Han L, Kariuki NN, Zhong CJ. Thermal activation of molecularly-wired gold nanoparticles on a substrate as catalyst. Journal of the American Chemical Society. 2002; 124: 13988–13989. DOI: 10.1021/ja028285y

[16] Che GL, Lakshmi BB, Fisher ER, Martin CR. Carbon nanotubule membranes for electrochemical energy storage and production. Nature. 1998; 393: 346–349. DOI: 10.1038/30694

[17] Hu JT, Min OY, Yang PD, Lieber CM. Controlled growth and electrical properties of heterojunctions of carbon nanotubes and silicon nanowires. Nature. 1999; 399: 48–51. DOI: 10.1038/19941

[18] Georgakilas V, Gournis D, Tzitzios V, Pasquato L, Guldi DM, Prato M. Decorating carbon nanotubes with metal or semiconductor nanoparticles. Journal of Materials Chemistry. 2007; 17: 2679–2694. DOI: 10.1039/B700857K

[19] Strano MS, Dyke CA, Usrey ML, Barone PW, Allen MJ, Shan HW, Kittrell C,. Hauge RH, Tour JM, Smalley RE. Electronic structure control of single-walled carbon nanotube functionalization. Science. 2003; 301(5639): 1519–1522. DOI: 10.1126/science.1087691

[20] Cao J, Sun JZ, Heng H, Li HY, Chen HZ, Wang M. Carbon nanotube/CdS core–shell nanowires prepared by a simple room-temperature chemical reduction method. Advanced Materials. 2004; 16(1): 84–87. DOI: 10.1002/adma.200306100

[21] Hickey SG, Riley DJ, Tull EJ. Photoelectrochemical studies of CdS nanoparticle modified electrodes: Absorption and photocurrent investigations. Journal of Physical Chemistry B. 2000; 104: 7623–7326. DOI: 10.1021/jp993858n

[22] Tessler N, Medvedev V, Kazes M, Kan SH, Banin U. Efficient near-infrared polymer nanocrystal light-emitting diodes. Science. 2002; 295(5559): 1506–1508. DOI: 10.1126/science.1068153

[23] Bechinger C, Ferrer S, Zaban A, Sprague J, Gregg BA. Photoelectrochromic windows and displays. Nature. 1996; 383: 608–610. DOI: 10.1038/383608a0

[24] Chen J, Lu G. Controlled decoration of carbon nanotubes with nanoparticles. Nanotechnology. 2006; 17: 2891–2894. DOI: 10.1088/0957-4484/17/12/011

[25] Banerjee S, Wong SS. Synthesis and characterization of carbon nanotube − nanocrystal heterostructures, Nano Letters. 2002; 2: 195–200. DOI: 10.1021/nl015651n

[26] Li W, Gao C, Qian H, Ren J, Yan D. Multiamino-functionalized carbon nanotubes and their applications in loading quantum dots and magnetic nanoparticles. Journal of Materials Chemistry. 2006; 16: 1852–1859. DOI: 10.1039/B600190D

[27] Robel I, Bunker BA, Kamat PV. Single-walled carbon nanotube–CdS nanocomposites as light-harvesting assemblies: photoinduced charge-transfer interactions. Advanced Materials. 2005; 17: 2458–2463. DOI: 10.1002/adma.200500418

[28] Paul R, Kumbhakar P, Mitra AK. A facile chemical synthesis of a novel photo catalyst: SWCNT/titania nanocomposite. Advances in Nano Research. 2013; 1(2): 71–82. DOI: 10.12989/anr.2013.1.2.071

[29] Yang MQ, Weng B, Xu Y-J. Synthesis of In_2S_3–CNT nanocomposites for selective reduction under visible light. Journal of Materials Chemistry A. 2014; 2: 1710–1720. DOI: 10.1039/C3TA14370H

[30] Shi Z, Liu C, Shen Lv W, Shen H, Wang D, Chen L, Li LS, Jin J. Free-standing single-walled carbon nanotube–CdSe quantum dots hybrid ultrathin films for flexible optoelectronic conversion devices. Nanoscale. 2012; 4: 4515–4521. DOI: 10.1039/C2NR30920C

IntechOpen